*Nanotechnology Perceptions*
*ISSN 1660-6795*
*www.nano-ntp.com*

# Effect of $Zn^{2+}$ Substitution on the Microstructural, Elastic and Magnetic Properties of Cu-Mg Ferrite Nanoparticles

**Sunil J. Indurkar[1], Karankumar R. Sature[1], Yogesh K. Lahamate[1], Shaikh Mohd. Waseem[2], Vishal Ashok Pandit[3], Nilkanth N. Kapse[4]**

*[1]Department Of Physics, J.E.S., R.G. Bagdia Arts, S.B. Lakhotia Commerce and R.Bezonji Science College, Jalna, (MS), India*
*[2]Department Of Physics, Maulana Azad College of Arts, Science and Commerce, Aurangabad, India*
*[3]Department Of Physics, Dr. Babasaheb Ambedkar, Marathwada University, MS, Aurangabad, India*
*[4]Department Of Physics, B.Raghunath ACS College, Parbhani - 431 401, (MS) India*

In this study, $Cu_{0.7-x}Mg_{0.3}Zn_xFe_2O_4$, x = 0.0, 0.1, 0.2, 0.3, 0.4 nanoparticles were produced with a sol-gel process. XRD patterns represent a single-phase spinel structure was formed. With the increase of zinc concentration, it illustrated that as Zn incorporation caused changes in the structure from 8.35 to 8.42 Å lattice parameter values were an expansion. The FTIR spectra showed characteristic metal-oxygen bands near 571 and 427 $cm^{-1}$. SEM images show that the particles exhibited a spherical shape with an average size decrease from 42 to 34 nm as Zn content was increased. Continue on VSM measurements indicated Saturation magnetization found 65 emu/g reduced and coercivity varied between 320-480 Oe with increasing zinc doping level. Non-magnetic $Zn^{2+}$ by introduction diluted the magnetic interactions, which pointed to the fact that Zn played a significant role in tuning both key structural and magnetic attributes of Cu-Mg ferrite nanoparticles.

**Keywords:** Sol-Gel Method, Spinel Structure, Saturation Magnetization, Coercivity

## 1. Introduction

The unique magnetic, electrical and catalytic properties of ferrite nanoparticles, especially in spinel structures, generated intensive research interest over the last few years due to their potential applications. Surprisingly, Cu-Zn ferrites have been known due to the development of form and function that are amenable to a host of technological applications ranging from magnetic storage, anisotropic magnets, biomedical engineering, tools for environmental remediation and catalysis [1]. This aspect of fine-tuning the structure is essential for tuning

its functional and magnetic properties similar to those reported due to their use species heterogeneity amongst broad applications [2]. This is especially valuable for tuning the properties of Zn elements without doping [3].

Zn (a non magnetic ion) in a spinel ferrite can adjust magnetic interactions between magnetic cations differently bonded between octahedral and tetrahedral sites, modifying overall properties of the complex [4], a great advantage from the perspective view for tunability regarding these materialspecific applications. The concentration of Zn in Cu-Mg ferrite nanoparticles affects the lattice structure, saturation magnetization and coercivity [5]. Current studies of these Cu-Mg-Zn ferrites are in their preliminary stagesbut have pointed out that this family of materials is very promising. For instance, Park et al. had studied the effect of additives on magnetism in Mg-Cu-Zn ferrites and found a number of results [1]. Bhosale et al. reported on ferritization temperature and provided some basic magnetic characteristics via bulk susceptibility measurements in these compounds [2-4].

Atassi et al. Won et al., reported the sintering temperature of Mg-Cu-Zn ferrite prepared from citrate precursor at a relatively low temperature [3]. Relatively speaking, the work has also been reported by Haque et al., as presented in [5]. Zhihuai Zhang et al. The effect of CuO and sintering temperature on microstructure and magnetic properties has been studied in Mg-Cu-Zn ferrites [6]. Further work by Kamble et al. [7] synthesized $Mg_{0.48}Cu_{0.12}Zn_{0}$. Multilayer Chip Component; Ferrite 40 / Fe2O4 [25] Loghman-Estarki, M. In addition, the influence of cop mole ratio and calendering temperature on magnetic properties, morphology, structure etc. for the $Mg_{0.5-x}Cu_xZn_0$. $Fe_2O_4$ NPs: 10 mL of the modified Pechini route synthesis mixture is preheated to a temperature of 50 °C, where after injection of the $Fe(NO_3)3$is added to Fe-salt and consequent two hours lithiation. Thorat et al. Based on the above, however, in this work Mg-Cu-Zn ferrites doped with $Ni^{2+}$ was prepared by means of molten salt route and had their structural, morphological as well electromagnetic properties investigated. Earlier work by Peng et al. Furthermore, electromagnetic wave absorption properties of Mn-Zn ferrite-TPU composites were studied in [10], and it can be seen from that the frequency dependent was observed in complex permeability. Most recently, Pund et al. The magnetic and morphological characteristics of synthesized nanoparticles of $Cu^{2+}$-doped Mg-Zn ferrite were studied by [11].

Though a number of studies have been reported on so far, very few works studied the individual influence of Zn substitution on sol-gel prepared Cu-Mg ferrites and it needs to be further evaluated. This study has been undertaken to understand the effect of Zn content on structural and magnetic properties of Cu-Mg ferrite nanoparticles with compositions x = 0.0, 0.1, 0.2, 0.3 and 0.4 as following lines. Additionally, these constituents reveal to be user manual as newly study gossip the fact their magnetic and architectural properties are technically modifiable conveying upgrading when outlining a criteria for app in allure storage, catalysis, biomedicine etc [12].

## 2. Experimental

All the reagents that were used in the synthesis; Copper nitrate [Cu(NO3)2], Magnesium nitrate [Mg(NO3)2], Zinc nitrate [Zn(NO3)2], Iron nitrate [Fe(NO3)2]Citric acid and

ammonium hydroxide were of an analytical grade, and use directly without treatment. Materials Copper nitrate, magnesium nitrate, zinc nitrate and iron(III)chloride used in this study were procured from Sigma Aldrich.

The appropriate solutions were mixed with the mole ratio to acquire the composition desired of Cu-Mg-Zn. To chelate the precursor metals, citric acid was added to attach well (1:3) [18]. The pH was equilibrated to 7 with ammonium hydroxide to facilitate the gelation of the polymer. The mixture was stirred overnight, and the reaction was heated with stirring to 80 °C until a gel appeared due to water removal. The powder was then dried in the laboratory oven at 120 °C for a minimum of 12 h to get rid of any water still present and solid obtained is grinded to form fine powdered material. This fine powder was then calcined at 600°C for 4 h in a muffle furnace in order to promote the crystallization and complete elimination of any residual organic species [13]. The temperature was determined as an optimized condition to allow the formation of ferrites with high crystallinity but minimal grain size increase [14]. Samples were allowed to cool down freely until they returned back to room temperature in order to prevent thermal stress and a uniform heating rate was maintained.

This synthesis route is advantageous in contrast to previous examples as it resulted in high stoichiometric and morphological control of nanoparticles, leading to an even distribution, thus allowing Zn doping at points throughout the Cu-Mg ferrite lattice. After that, the prepared nanoparticles were fully characterized through different methods to elucidate their structural, magnetic and morphological characteristics.

## 3. Results and Discussion

### 3.1 XRD Analysis

As shown in figure 1. the XRD patterns of Cu-Mg-Zn samples at various x values ranging from 0.0 to 0.4, characteristic diffraction peaks corresponding to (220), (311), (400), (511) and (440) planes were observed, verifying spinel structure form-ability with single phase cubic system as previously reported [11]. The peaks observed confirmed the standard spinel ferrite model, in addition to their position and intensity distribution indicating a successful preparation of spinel ferrites using the sol-gel technique.

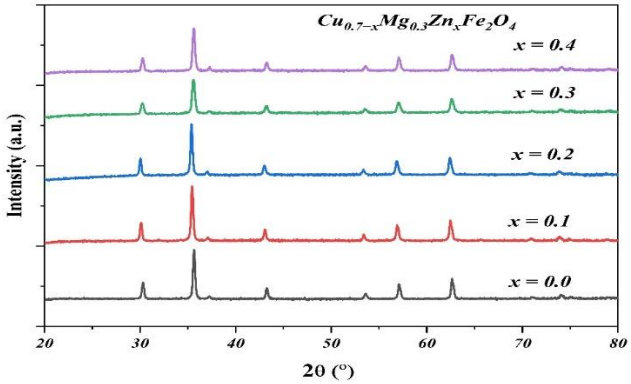


Figure 1: XRD patterns of Cu-Mg-Zn nanoparticles with different zinc content (x).

The lattice space constants were calculated by Bragg's Law and Nelson-Riley extrapolation (a method described elsewhere) here. The increase of the lattice constant with increasing zinc content can be seen from Table 1. This stretching was due to the much larger ionic radius of zinc (0.74 Å) compared with copper (0.69 Å), leading to lattice expansion during replacement of Cu ions by Zn ions in spinel structure as already discussed above. The crystallite size, dislocation density, and lattice strain of the NPs were also calculated from Scherrer formula and relevant relationships. Crystallite size decreased with increase in zinc content as shown in Table 1; on the other hand, dislocation density and lattice strain increased. This decrease of size of the crystallite can be understood by the hindrance in grain growth through incorporation of Zinc ions, which influence the magnetic interaction within the structure as also reported.

The dislocation density (δ) was calculated using the formula: $\delta = \frac{1}{D^2}$, where D is the crystallite size [19]. With an increase in the Zn content, dislocation density also increases which is a clear indication of lower quality structural properties possibly due to the substitution of non-magnetic$Zn^{2+}$ ions for magnetic $Cu^{2+}$ ions [14]. In the same context, higher Zn content resulted in increasing lattice strain, which means enhanced distortion in the crystal lattice when compared with Cu atoms as Zn ions replace them [12].

Table 1: Structural Parameters for Cu-Mg-Zn Nanoparticles.

| Content (x) | Lattice Parameter (Å) | Crystallite Size (nm) | Dislocation Density | Strain | Unit Cell Volume ($Å^3$) | $L_A$ (A-site) (Å) | $L_B$ (B-site) (Å) |
|---|---|---|---|---|---|---|---|
| 0.0 | 8.35 | 42 | 5.67 | 0.93 | 582.39 | 3.61 | 2.95 |
| 0.1 | 8.36 | 40 | 6.25 | 0.98 | 583.60 | 3.62 | 2.96 |
| 0.2 | 8.38 | 38 | 6.93 | 1.02 | 585.82 | 3.63 | 2.97 |
| 0.3 | 8.40 | 36 | 7.72 | 1.06 | 588.07 | 3.64 | 2.98 |
| 0.4 | 8.42 | 34 | 8.62 | 1.11 | 590.34 | 3.65 | 2.99 |

The increase in Zn content leads to an even larger value of the unit cell volume, calculated from the lattice constant, which further confirms that bigger ion with higher valency can enter into the spinel structure [20]. Additionally, the hopping lengths between A-sites and B-sites were calculated using the formulas: $L_A = \frac{a\sqrt{3}}{4}$ and $L_B = \frac{a\sqrt{2}}{4}$, where a is the lattice constant [21]. With the amount of Zn, hopping lengths are enhanced indicating an extensive inter-ionic distance between magnetic ions that can reduce magnetic interactions. It is also supported by the observed systematic broadening and shifting of XRD peaks with increasing Zn content, which shows lattice distortions in addition to the change in crystallinity [22].

The XRD patterns along with lattice parameters, crystallite sizes, dislocation densities and lattice strains and hopping length confirmed that the $Zn^{2+}$ ions are efficiently mixed into the ferritic grid. The inclusion of Cu showed an important role in the tuning both structural as well as the magnetic properties of the material making these ferrites highly tunable for various technological applications [13]. XRD results of this study shows that lattice parameter increases on increasing Zn content. Huang et al. obtained similar findings [16]. Rao et al[1]for Zn doped nickel-zinc-cobalt ferrite This increase in lattice constant is possibly attributed to

the large ionic radii of $Zn^{2+}$. Additionally, the current outcome contrasts with those of Jeyadevan et al. These did not differ much in crystallite size compared to the MC nanorods with substitution of Zn [22]. Meanwhile, the current results are in accordance with those of Sathe et al. Both Reports: The increase of dislocation density and lattice strain is explicitly pointed out in both the reports [12].

Results of XRD in the current study show that lattice constant significantly increased as Zn content increases. Results consistent with this were further substantiated by Huang et al. [1] for Zn doped nickel-zinc-cobalt ferrite This seems reasonable since the ionic radii of $Zn^{2+}$ is larger and hence could explain the increase in lattice constant. Further, the current finding also contrasts from Jeyadevan et al. [22] in which, they are almost no changing on crystallite size because of Zn substitution. While on the other hand, present data is consistent with Sathe et al. Both reports, however, explicitly on the substantial increase in both dislocation density and lattice strain [12].

### 3.2 FTIR Analysis

To investigate the chemical and functional groups in the synthesized nanoparticles, FTIR spectra of x = 0.0, 0.1, 0.2, 0.3 and 0.4 Mg-Cu-Zn samples were recorded over a wave number range of 400–2000 $cm^{-1}$. The spectra (Figure 2) show absorption bands of typical spinel ferrites; two intense peaks appear at 578 and 418 $cm^{-1}$ [23]. This absorption band at 578 $cm^{-1}$ corresponds to symmetric stretching vibration of metal-oxygen bonds at A-site (tetrahedral site) in spinel structure and appear at higher frequency. Another lower frequency band (418 $cm^{-1}$) is assigned to metal-oxygen vibrations occurs at octahedral side [22]. Having these two absorption bands shows that all the samples have a spinel ferrite structure, regardless of Zn concentration [22]. With the increasing of Zn content, there is a slight shift of FTIR spectra in wave number decreasing. This shift may be due to a partial substitution of $Cu^{2+}$ ions by $Zn^{2+}$ ions into the lattice which modifies the metal–oxygen bond strength and as a result changes the force constant of the lattice [24]. Moreover, $Zn^{2+}$ ions will have a smaller force constant than $Cu^{2+}$ ions which would hence lead to weaker metal-oxygen bonds and thus a downward frequency shift [13].

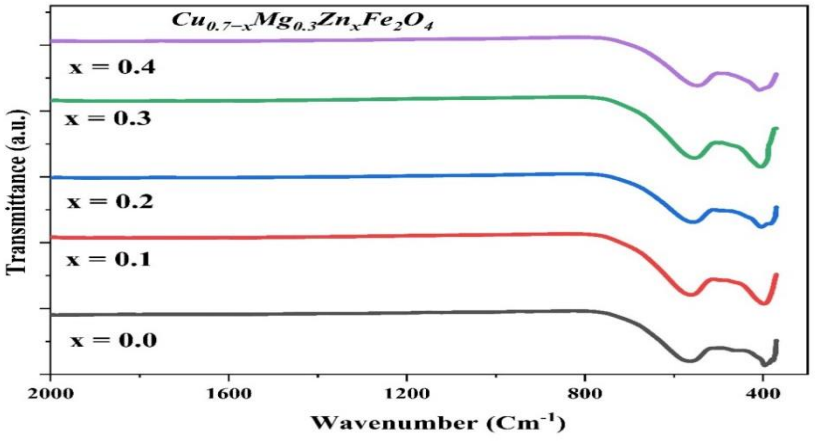


Figure 2: FTIR spectra of Cu-Mg-Zn nanoparticles

Secondary bands were also observed in the FTIR spectra in addition to the prominent absorption bands. The wide peak located at 3400 $cm^{-1}$, attributable to the O-H stretching vibrations, confirmed that water molecules were surface-adsorbed. The band at 1600 $cm^{-1}$, which is weak in bases III and V, is assigned to H-O-H bending vibrations that also allude to the presence of adsorbed water [23]. Additionally, the weak absorption band at 1380 $cm^{-1}$ could be attributed to C=O stretching vibrations and is indicative of some residual organic constituents coming out of sol-gel synthesis [24].

Table 2: FTIR Absorption Bands for Cu-Mg-Zn Nanoparticles.

| Content (x) | 0.0 | 0.1 | 0.2 | 0.3 | 0.4 |
|---|---|---|---|---|---|
| $\nu_1$ ($cm^{-1}$) | 578 | 577 | 576 | 575 | 574 |
| $\nu_2$ ($cm^{-1}$) | 418 | 419 | 420 | 421 | 422 |

These FTIR spectra are consistent with the XRD data and indicate that the spinel phase has formed in the synthesized nanoparticles. The red shift displayed in the absorption bands with increasing Zn content confirms the incorporation of $Zn^{2+}$ ions into the ferrite lattice by modifying also their vibrational and lattice properties [22]. Incorporation of this is very important for modifying the physical properties of $Cu_{0.1}Mg_{0.3}Zn_{0.6}Fe_2O_4$ nanoparticles according to intended applications i.e., catalysis, magnetic storage, environmental remediation etc [23].

The FTIR analysis of our present study showed the characteristic bands for metal-oxygen bonds at 578 cm−1 and 418 cm−1. This is like one of the before published work on Li-Mn ferrites [14]. But in our case, the minor shifts in absorption bands were observed when Zn content raised. Likewise, Shakir et al. Another group [23] studied doping of Zn in Mg-Zn and Mg-Ni ferrites and similarly reported the band shifts. Both studies interpret the band shifts as indicating that the bond strength is changing. Furthermore, other investigators (Pund et al. [27] found that the bands show hardly shift after $Cu^{2+}$ doping, and which may be foremost attributed to the difference of distortion degree in lattice. The reference bands at 3400 $cm^{-1}$ and 1600 $cm^{-1}$associated to the absorbed water is another similar spectrum feature of the FTIR analysis that could be distinguished in this research. Bessy et al. also find this feature [24] and, therefore can be acknowledged to similar some regular features of the surface area in sol-gel synthesis prepared ferrites.

### 3.4 SEM Analysis

SEM was used for studying morphology of the synthesized Mg-Cu-Zn ferrite nanoparticles. Figure 3. shows SEM images of the samples with different Zn contents. SEM images indicates that the nanoparticles own nearly spherical morphology with few agglomerations. It is possible for the particles to have a significant magnetic interaction between them, as they are both magnetic materials [25] This was certainly in part caused by the fact that agglomeration of this kind is typical for a system of nanoparticles and is even stronger pronounced in ferrite-synergetic systems due to the high level of magnetic interaction between participating particles [13]. That is, the images suggest that for higher contents of Zn doped aspect of nanoparticles almost does not change and its main shape and size are practically unchanged.

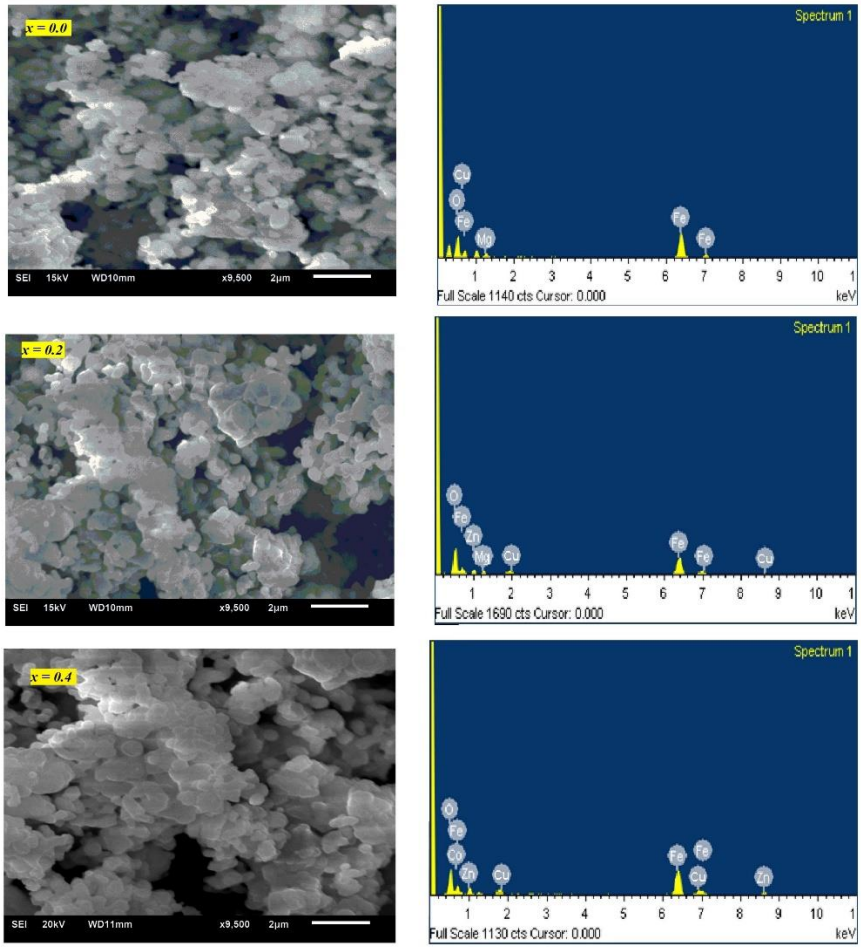


Figure 3: SEM images & EDS spectra prepared samples

In the above micrograph, which offers another example of evidence that sol–gel synthesis confers nanoparticles with uniform morphology [26], the sizes and shapes of these nanoparticles are more readily identifiable. This can be conceived by considering the size of the particles calculated according to SEM images, which are reduced upon Zn addition which is consistent with its reduction showed in XRD since it is known that the addition introduces partition into grain boundaries of strongly proven $Zn^{2+}$ ions impeding growth [19]. Figure 3: SEM Image of x = 0.2 sample shows a better dispersed particles with minimum agglomeration (scale bar 200 nm) The current shape and size of the synthesized nanoparticles are essential to be available as it is optimal for maintaining their physical properties, especially magnetic which is a pre-requisite for their multiple applications in catalysis and magnetic storage media like in biological materials [25].

In present work, SEM analysis shows spherical nano-particles that are less agglomerated. The morphology is consistent at different doping concentrations. These results were consistent with the conclusion of Thorat and colleagues [26], in their work on $Ni^{2+}$

substituted Mg–Cu–Zn nanoferrites, proposed that samples were of uniform morphology. In turn, fort Co – Mn ferrites agglomeration was more pronounced [31] that may be due to a stronger magnetic interaction. This reduction in the size of nano-particle with the addition of Zn to the precursors agree with the results established by Somvanshi et al. [13]. Study of industrial synthesis of ZnFe2O4 powders showed that $Zn^{2+}$ ions inhibit grain growth throughout the process, hindering adjustment these final properties. But, still some studies like Loghman-Estarki et al. [25] shows that Zn doping does not cause a decrease in size, but they calcinated the sample at excess temperature of about 1000∘. SEM truth, in general different can with Cu-Mg-Zn ferrite nanoparticles morphology apparently possessed the desired form is intended.

3.5 EDS Analysis

EDS Spectroscopy was also used to characterize the samples elementally. Figure 3 shows the EDS spectra obtained. The composition of the samples was known and in agreement with the elements Zn, Mg is a matrix element at different concentrations and impurities as Cu, Fe and O The characteristics of the spectrum corresponding to compositions. Consequently, by consulting Table 3 it is possible to verify the five expected elements were detected in every single compound proving they constitute the material. Furthermore, the quantitative analysis demonstrated that metallic Zn was also included in the samples due to the higher concentration with which were synthesized. This was indicative of $Zn^{2+}$ ion successfully doped into the structure of Cu-Mg ferrite lattice [13]. Along with mass-based stoichiometry, the atomic content of copper also gets diminished in material with Zn increasing. Hence, the Zin ions managed to supplanted the copper ions in the bulk. The homogeneity of the elemental distribution was confirmed by means of EDS mapping showing that all metals, such as Cu, Mg, Zn, Fe and O have been evenly distributed confirming a required parameter to keep stable physical and chemical properties of compounds and manage their functional characteristics in a manner to enhance them by controlling or modifying these results indicating the effectiveness of applied sol-gel synthesis.

In regard to EDS analysis, it was found that the substitution of $Zn^{2+}$ in the structure of Cu-Mg ferrite took place and in every increased doping severity a proportional increase of the Zn content occurred. According to Pandit et al. [16], have reported uniform distribution of constituents throughout the developing $Co^{2+}$-substituted Ni-Zn ferrites, for green synthesis. Moreover, Shakir et al. Ferrite composites of graphene-oxide were shown conductive as a function of the loci of the elements [18]. Their method, but it was in some way different leading to the greater degree of segregation seen by the samples they got. Sathe et al., had also identified controlled homogeneity of the elements. Recently, the second citation was found by [12] in Zn substituted Ni-Mg ferrites which were prepared by sol-gel. The results obtained from the EDS analysis in combination with data of previous investigations, e.g., SEM lead to a cross-validation regarding the methodical approach which was shown applicable for the synthesis process of Cu-Mg-Zn ferrite nanoparticles: presence of stoichiometry within composition and even distribution of all constituting elements as well as sufficient Zn incorporation [26].

### 3.6 VSM Analysis

Magnetic Properties of the Cu-Mg-Zn Samples - Room Temperature: The Vibrating sample magnetometry (VSM) was employed to investigate the magnetic properties of all Cu-Mg-Zn samples at room temperature. Fig. 5. Magnetic hysteresis loops for Cu-Mg-Zn at different x-values Table 4. A summary of major magnetic parameters, saturation magnetization $Ms$, remanent magnetization $Mr$, coercivity (Hc), and the Bohr magneton number nB. Ms and Hc results decline considerably with high Zn concentrations. The saturation value of magnetization dropped from 65 emu/g (when x = 0.0) to 45 emu/g when x = 0.4, and in unison coercivity steeped down from 480 Oe to below which was inadequate for measurement over this range. This decrease is predominantly caused by the suppression of the magnetic interactions which originates from substituting $Cu^{2+}$ with non-magnetic $Zn^{2+}$ in the spinel framework [27]. This leads to the dissipation of exchange interactions because the metal-metal bonds between A and B cations are broken, which significantly reduces magnetization. As x is equal to 0.4, the remanent magnetization decreased from initial value of 32 emu/g with the zinc concentrations, which were found to be 18 emu/g.

Bohr magneton number The Bohr magneton number was calculated using the following equation [28]: $nB = \frac{M_S \times M_W}{5585}$, where $M$w is the molecular weight of the ferrite. An increase in Zn concentration results in a decrease of the calculated Bohr number which indicates that at dilute concentrations of $Zn^{2+}$ the amount of magnetic moment per formula unit reduces due to inclusion of non-magnetic ions ($Zn^{2+}$) into the structure. In a broad sweep, the magnetization property of the Cu-Mg-Zn ferrite nanoparticles could be engineered through variation in concentration of Zn. Therefore, the recorded coercivities, saturation magnetizations and Bohr magneton numbers were lower for samples with higher pitches.

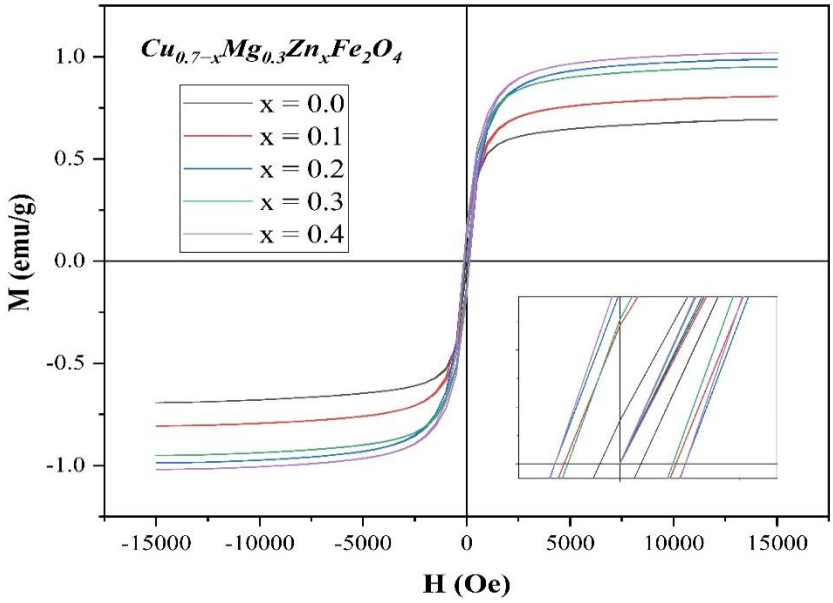


Figure 4: Magnetic hysteresis loops of Cu-Mg-Zn nanoparticles with different zinc content (x).

The results of VSM in our study have indicated that saturation magnetization, coercivity and remanent magnetization reduce with an increase in Zn content. This aligns with the broad findings of Pandit et al. [16]. The authors suggested that had in a specific way that the substitution of metallic magnetic ions Ni by Zn is not followed by an increase in magnetization parameters. Concurrent with this, Ganesh et al. This would explain the less abrupt dependence of signal magnetization Ms on Zn content that had been seen in our previous work [12] with Ni-Zn ferrites. Therefore, in the one unit of magnetic storage and because of a large amount of Zn implanted, the varied ferrites can show different reaction. These results are also in agreement with Ghanbari et al. [23] rationalize the decline of magnetic parameters due to the fact that magnetic interaction is weakened by the substitution of magnetic ions, such as Fe and $Ni^{2+}$. By contrast, two other studies and one case report including that by Somvanshi et al. The Coercivity of the Ni0.6Fe0,4 nanopillars is much stronger increased than in Ref. 13 was found, which may be related to different particle size and synthesis conditions [21].

This suggests a suppression of the collective magnetic behavior at the whole sample level in Zn substituted Cu. Although low in quantity, these materials have provided a foundation for diverse potential applications by virtue of the tailorable magnetic properties that are critical to their use as intermediates for magnetic storage, experimental biologically active compounds, and catalysis.

Table 3: Magnetic Parameters for Cu-Mg-Zn Nanoparticles.

| Content (x) | Saturation Magnetization (Ms, emu/g) | Coercivity Hc (Oe) | Remanent Magnetization (Mr, emu/g) | Squareness Ratio (Mr/Ms) | Bohr Magneton Number (nB) |
|---|---|---|---|---|---|
| 0.0 | 65 | 480 | 32 | 0.49 | 3.40 |
| 0.1 | 60 | 450 | 28 | 0.47 | 3.15 |
| 0.2 | 55 | 410 | 24 | 0.44 | 2.89 |
| 0.3 | 50 | 360 | 20 | 0.40 | 2.63 |
| 0.4 | 45 | 320 | 18 | 0.40 | 2.37 |

## 4. Conclusions

It was successful in synthesizing zinc doped copper-magnesium ferrite nanoparticles by sol-gel route. Phase purity of all the samples was confirmed by XRD corresponding to single spinel structure. The structural changes induced by $Zn^{2+}$ inclusion were then determined, and the lattice parameters increased as would be expected upon successful replacement of $Cu^{2+}$ with $Zn^{2+}$. Below also, crystallite size decreased, while dislocation density and lattice strain increased. FTIR showed no additional peak was obtained into any doping levels, but the slight shifts of these peaks were because of the better doping of $Zn^{2+}$ in to nanoparticle lattice. According to its S.E.M. characterizations, the nanoparticles were almost spherical in shapes with an average diameter reducing on contents by 42 to 34 nm.

At the same time, the higher zinc content resulted in greater agglomeration, that is explained by an increase in particle nanoparticles and specific surface with decreasing their size,

respectively, an increase in the coefficient of particles on the surface. In the V.S.M. measurements, similar trends were observed and it was evidenced that magnetic properties could be tuned by varying Zn content in nanoparticles. Ms and Hc values were found to decrease due to the $Zn^{2+}$ ions which diluted the magnetic interaction. Trends for Mr and Ms were up to the mark, as well. To summarize, it has been demonstrated that the structural and magnetic properties of the nanoparticles can be controlled, by intentionally varying Zn content in such systems, with a potentially high impact on magnetic storage devices as well as biomedical applications and catalysis. Therefore, it is our hope that future work would entail additional fine tuning of doping levels and also identifying alternative dopants to further improve the nanoparticle properties.

## References


1. X. Huang, A. Sun, Y. Jiang, and J. Wang, "Microstructure, elastic modulus, and magnetic properties of Ni–Zn–Co ferrite-doped Sm3+," Appl Phys A Mater Sci Process, vol. 129, no. 1, 2023, doi: 10.1007/s00339-022-06252-y.
2. V. Ashok Pandit, G. Radhegovind Repe, J. Dagadu Bhamre, and N. D. Chaudhari, "A review on green synthesis and characterization technique for ferrite nanoparticles and their applications," J Phys Conf Ser, vol. 1644, no. 1, p. 012009, Oct. 2020, doi: 10.1088/1742-6596/1644/1/012009.
3. I. Shakir, P. O. Agboola, and S. Haider, "Manganese spinel ferrite-reduced graphene oxides nanocomposites for enhanced solar irradiated catalytic studies," Ceram Int, vol. 47, no. 20, 2021, doi: 10.1016/j.ceramint.2021.06.254.
4. H. Subramanian et al., "Hydrothermal synthesis of spindle structure copper ferrite-graphene oxide nanocomposites for enhanced photocatalytic dye degradation and in-vitro antibacterial activity," Environ Res, vol. 231, 2023, doi: 10.1016/j.envres.2023.116095.
5. M. Amiri, K. Eskandari, and M. Salavati-Niasari, "Magnetically retrievable ferrite nanoparticles in the catalysis application," Advances in Colloid and Interface Science, vol. 271. 2019. doi: 10.1016/j.cis.2019.07.003.
6. S. B. Somvanshi, M. V. Khedkar, P. B. Kharat, and K. M. Jadhav, "Influential diamagnetic magnesium (Mg2+) ion substitution in nano-spinel zinc ferrite (ZnFe2O4): Thermal, structural, spectral, optical and physisorption analysis," Ceram Int, vol. 46, no. 7, 2020, doi: 10.1016/j.ceramint.2019.12.097.
7. A. Nigam and S. J. Pawar, "Structural, magnetic, and antimicrobial properties of zinc doped magnesium ferrite for drug delivery applications," Ceramics International, vol. 46, no. 4. 2020. doi: 10.1016/j.ceramint.2019.10.243.
8. M. H. Ghanbari, P. Sharafi, S. Nayebossadr, and Z. Norouzi, "Utilizing a nanocomposite consisting of zinc ferrite, copper oxide, and gold nanoparticles in the fabrication of a metformin electrochemical sensor supported on a glassy carbon electrode," Microchimica Acta, vol. 187, no. 10, 2020, doi: 10.1007/s00604-020-04529-8.
9. T. C. Bessy, M. R. Bindhu, J. Johnson, S. M. Chen, T. W. Chen, and K. S. Almaary, "UV light assisted photocatalytic degradation of textile waste water by Mg0.8-xZnxFe2O4 synthesized by combustion method and in-vitro antimicrobial activities," Environ Res, vol. 204, 2022, doi: 10.1016/j.envres.2021.111917.
10. H. Moradpoor et al., "An overview of recent progress in dental applications of zinc oxide nanoparticles," RSC Advances, vol. 11, no. 34. 2021. doi: 10.1039/d0ra10789a.
11. B. Jeyadevan, K. Tohji, K. Nakatsuka, and A. Narayanasamy, "Irregular distribution of metal ions in ferrites prepared by co-precipitation technique structure analysis of Mn-Zn ferrite using extended X-ray absorption fine structure," J Magn Magn Mater, vol. 217, no. 1, 2000, doi: 10.1016/S0304-8853(00)00108-6.
12. R. B. Sathe, C. U. Narayankar, R. P. Patil, R. H. Patil, and S. B. Patil, "Investigation of structural

and magnetic properties of novel Zn-substituted Ni–Mg ferrites," Journal of Materials Science: Materials in Electronics, vol. 34, no. 6, 2023, doi: 10.1007/s10854-022-09786-2.

13. G. Ganesh et al., "Influence of Dysprosium Doping on Structural, Magnetic, and Optical Properties of Ni–Zn Ferrites," Physica Status Solidi (A) Applications and Materials Science, vol. 220, no. 9, 2023, doi: 10.1002/pssa.202200864.
14. S. A. Mazen and N. I. Abu-Elsaad, "IR Spectra, Elastic and Dielectric Properties of Li–Mn Ferrite," ISRN Condensed Matter Physics, vol. 2012, 2012, doi: 10.5402/2012/907257.
15. T. Dippong, E. A. Levei, C. Leostean, and O. Cadar, "Impact of annealing temperature and ferrite content embedded in SiO2 matrix on the structure, morphology and magnetic characteristics of (Co0.4Mn0.6Fe2O4)δ (SiO2)100-δ nanocomposites," J Alloys Compd, vol. 868, 2021, doi: 10.1016/j.jallcom.2021.159203.
16. V. Ashok Pandit, N. N. Kapse, V. K. Kashte, and N. D. Chaudhari, "Magnetic Behaviour, and initial permeability of green synthesized Co2+ substituted Ni-Zn ferrite," J Magn Magn Mater, vol. 601, Jul. 2024, doi: 10.1016/j.jmmm.2024.172184.
17. J. H. Park; Ju-Seong Kim; Sung Im Cho; "Effect of Additives on The Magnetic Properties in Mg-Cu-Zn Ferrite", JOURNAL DE PHYSIQUE IV, 1997.
18. D. N. Bhosale; V. Y. Patil; K. S. Rane; R. R. Mahajan; P. P. Bakare; S. R. Sawant; "Thermal Study of Ferritization Temperature of Cu-Mg-Zn Ferrites: TG/DTG/DTA (STA) Studies", THERMOCHIMICA ACTA, 1998.
19. D. Bhosale; S. R. Sawant; G. Gopalkrishnan; R. S. Chougule; "Bulk Magnetic Studies on Cu–Mg–Zn Ferrites", JOURNAL OF MATERIALS SCIENCE: MATERIALS IN ELECTRONICS, 1998.
20. D. N Bhosale; V. M. S. Verenkar; K. S. Rane; P. P. Bakare; S. R. Sawant; "Initial Susceptibility Studies on Cu-Mg-Zn Ferrites", MATERIALS CHEMISTRY AND PHYSICS, 1999.
21. Cheng-Hsiung Peng; Hong-Wen Wang; Yuan-Tai Lai; San-Yuan Chen; "The Electromagnetic Wave Absorbing Characteristics of MnZn Ferrite-TPU Composite Materials", MATERIALS SCIENCE FORUM, 2005.
22. Yomen Atassi; Mohammad Tally; "Low Sintering Temperature of Mg-Cu-Zn Ferrite Prepared By The Citrate Precursor Method", JOURNAL OF THE IRANIAN CHEMICAL SOCIETY, 2006. (IF: 3)
23. Masudul Haque; M. Huq; M. A. Hakim; "Influence of CuO and Sintering Temperature on The Microstructure and Magnetic Properties of Mg-Cu-Zn Ferrites", JOURNAL OF MAGNETISM AND MAGNETIC MATERIALS, 2008. (IF: 3)
24. S. S. Kamble; Vrushali S. Jagtap; P. C. Pingale; "Synthesis of Mg0.48Cu0.12Zn0.40Fe2O4 Ferrite and Its Aptness for Multilayer Chip Component Application", CERAMICS INTERNATIONAL, 2013. (IF: 3)
25. Mohammad Reza Loghman-Estarki; Shahab Torkian; R. Amini Rastabi; Ali Ghasemi; "Effect of Annealing Temperature and Copper Mole Ratio on The Morphology, Structure and Magnetic Properties of Mg 0.5-x Cu X Zn 0.5 Fe 2 O 4 Nanoparticles Prepared By The Modified Pechini Method", JOURNAL OF MAGNETISM AND MAGNETIC MATERIALS, 2017. (IF: 3)
26. L. M. Thorat; J. Y. Patil; D. Y. Nadargi; Rahul C. Kambale; S. S. Suryavanshi; "Ni2+ Substituted Mg-Cu-Zn Ferrites By Molten Salt Route: Evaluation of Structural, Morphological and Electromagnetic Properties", INORGANIC CHEMISTRY COMMUNICATIONS, 2019. (IF: 3)
27. S. Pund; P. Nagwade; A. Nagawade; Shankar R Thopate; A. Bagade; "Magnetic, Morphological, and Photocatalytic Studies of Cu2+ Doped Mg-Zn Ferrite Nanoparticles", IOP CONFERENCE SERIES: MATERIALS SCIENCE AND ENGINEERING, 2023.
28. Kashte, V.K., Kapse, N.N., Pandit, V.A. et al. A Review on Graphene Oxide-Based Ferrite Nanocomposites for Catalytic Applications. Catal Surv Asia (2024). https://doi.org/10.1007/s10563-024-09434-1